Formation of Monodisperse Microbubbles in a Microfluidic Device

J. H. Xu, S. W. Li, G. G. Chen, and G. S. Luo
The State Key Lab of Chemical Engineering, Dept. of Chemical Engineering, Tsinghua University, Beijing 100084, China

DOI 10.1002/aic.10824
Published online March 21, 2006 in Wiley InterScience (www.interscience.wiley.com).

The crossflowing rupture technique was first used in a microfluidic device to prepare microbubbles, and successfully prepared monodisperse microbubbles with polydispersity index (σ) values of <2%. The parameters affecting the microbubble-formation process, such as two-phase flow rates, continuous-phase viscosity, surface tension, and surfactants were investigated. The microbubble-formation mechanisms of the crossflowing rupture technique with those of the techniques of both flow-focusing rupture and geometry-dominated breakup were also compared. It was also found that the bubble size decreased with increasing continuous-phase rate and its viscosity, while independent of surface tension. The different species of surfactants also influenced the microbubble-formation process. Moreover, the bubble-formation mechanism by using the crossflow rupture technique was different from the techniques of both hydrodynamic flow focusing and geometry-dominated breakup. The microbubble-formation process using the crossflowing rupture technique is controllable. © 2006 American Institute of Chemical Engineers *AIChE J,* 52: 2254–2259, 2006

Keywords: monodisperse microbubbles, crossflowing rupture technique, microfluidic device

Introduction

Microbubbles have countless applications in science and technology. For example, fundamental medical applications of micron-size bubbles range from ultrasound contrast agents to thrombus destruction, targeted drug delivery, tumor destruction, and even as a flotation column.[1-5] In addition, intravenous injection of a stabilized solution of sufficiently small bubbles might be used in acute lung dysfunction. The control of bubble size and its distribution is critical in all these applications. Monodisperse microbubbles are more useful for fundamental studies because the interpretation of experimental results is much simpler than that of polydispersed microbubbles. They can also serve as useful systems for measuring important properties of microbubbles. For instance, the stability of microbubbles can be conveniently monitored. Monodisperse microbubbles can also greatly reduce Ostwald ripening by reducing the effective Laplace pressure difference because the bubbles size is uniform.

Recently, the growing trends in the miniaturization of experimental systems and the development of advanced functional materials have facilitated applications of micromachining techniques in various fields, such as microanalysis, on-chip separation, protein crystallization, and microchemical reaction.[6-9] The control of small volumes of fluids and understanding of multiphase flows are required in microfluidic devices. Liquid–liquid dispersions in microfluidic devices have been generated by a number of methods, including both geometry-dominated breakup,[10] crossflow rupturing through microchannel arrays,[11] hydrodynamic flow focusing through a small orifice,[12,13] and two-phase crossflowing rupture streams in T-junction microchannels.[7-9,14-16] Furthermore, highly uniform emulsion droplets with polydispersity index (σ) < 5% can alternatively be generated.[10,13,14] These investigators found that droplet formation of the dispersed phase was affected by all the parameters relevant to the drag force of the continuous phase

Correspondence concerning this article should be addressed to G. S. Luo at gsluo@tsinghua.edu.cn.

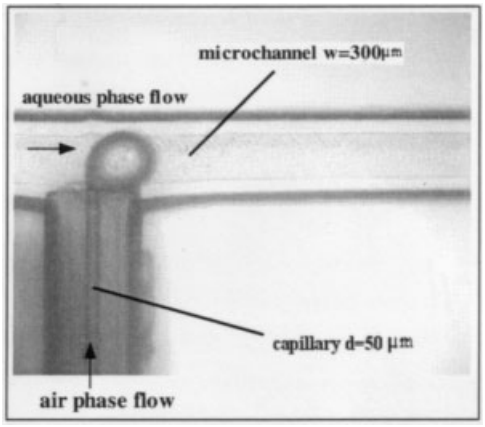

Figure 1. Micrograph of the cross section of microfluidic device.

and the momentum of the dispersed phase, such as flow rates, viscosities, and the interfacial tension. Although fewer studies have dealt with gas–liquid dispersions, Ganan-Calvo et al.[17] first described the formation of monodisperse gas bubbles in capillaries by using the hydrodynamic flow-focusing method. Garstecki et al.[18,19] described a flow-focusing device incorporated directly into a microfluidic chip that was capable of delivering monodisperse bubbles at frequencies exceeding 10^5 bubbles per second. In their work, the bubbles were highly uniform and σ was $<2\%$. Yasuno et al.[20] reported monodisperse microbubble formation using the method of geometry-dominated breakup in a microchannels (MCs) plate. From their work, the microbubble formation appears to be based on the spontaneous transformation caused by surface tension; moreover, the bubble size was affected by viscosity and the dispersing agents, but independent of the interfacial tension. However, microbubble formation by the crossflowing rupture technique in T-junction microchannels has not yet been reported.

In the present work, we attempt to form monodisperse microbubbles using the crossflowing rupture technique in a microfluidic device. We investigate the parameters affecting microbubble formation, such as two-phase flow rates, continuous-phase viscosity, surface tension, and surfactants. We also compare crossflowing rupture microbubble formation with the processes of both flow-focusing rupture and geometry-dominated breakup.

Experimental

Microfluidic device

The experiments were performed in a T-junction microchennel device fabricated on a thin plate ($100 \times 20 \times 5$ mm) of polymethyl methacrylate (PMMA) using an end mill (kindly provided by the Dept. of Biological Sciences and Biotechnology, Tsinghua University, Beijing, China). Figure 1 shows the micrograph of the T-junction section of the microfluidic device. The continuous (aqueous) phase flow channel dimensions are approximately 300×200 μm (width $\times$ height). A quartzose capillary with inner diameter of 50 μm was embedded into the vertical channel [200×200 μm (width $\times$ height)] as the gas flow channel and the microfluidic device was sealed using another PMMA thin plate of 1 mm thickness by using a high-pressure thermal sealing technique. Two microsyringe pumps and two gastight microsyringes were used to pump the two phases into the microfluidic device, respectively.

Materials

Air was used as the dispersed phase. Deionized water was used as the continuous phase. Different concentrations of sodium dodecyl sulfate (SDS) or polyoxyethylene (20) sorbitan monolaurate (Tween 20) used as the surfactants were added to the aqueous phase. SDS concentrations ranged from 0.01 to 0.5 wt % to control the interfacial tension between the aqueous phase and the air phase. Tween 20 concentrations of 1.0 and 2.0 wt %, which exceed the critical micelle concentration (CMC), were used to investigate the effect of surfactants on the microbubble-formation process. Glycerol was used to control the viscosities of the aqueous phase; in our experiments, three different glycerol concentrations of 24, 52, and 62 wt % were used. The properties of the experimental system are listed in Table 1.

Visualization and analysis

Experiments were carried out with a microscope at magnifications of $\times 100$. A high-speed CCD video camera was connected to the microscope and the images were recorded with a frequency of 200 images per second. The bubble-formation processes under different conditions were analyzed from microscope images. The size and distribution of microbubbles were recorded using the same microimaging system in a glass slide when the fluids flowed out onto it. After changing any of the flow parameters, we allowed at least 100 s of equilibration time. The average bubble size (d_{av}) and the polydispersity index (σ) were determined by measuring the sizes of at least 100 microbubbles from recorded pictures using custom-made image-analysis software. σ is defined by the following equation

$$\sigma = \delta / d_{av} \times 100\% \tag{1}$$

where σ is the polydispersity index, δ is the standard deviation, and d_{av} is the average bubble diameter.

Results and Discussion

Monodisperse microbubble formation and its distribution

The possibility of monodispersed microbubble formation was tested by pumping the air and the aqueous phase into the capillary and continuous-phase flow channel, respectively. Figure 2 shows four pictures of the bubble-formation process in the microchannel device under two different experimental con-

Table 1. The Experimental System

Continuous Phase	Surface Tension γ (mN m^{-1})	Viscosity, μ (mPa · s)
0.01–0.5% SDS/water	55.0–31.0	0.92
1% Tween 20/water	39.7	0.92
2% Tween 20/water	37.0	0.92
0.5% SDS/24% glycerol aqueous solution	30.3	2.0
0.5% SDS/52% glycerol aqueous solution	30.3	6.4
0.5% SDS/62% glycerol aqueous solution	30.3	10.84

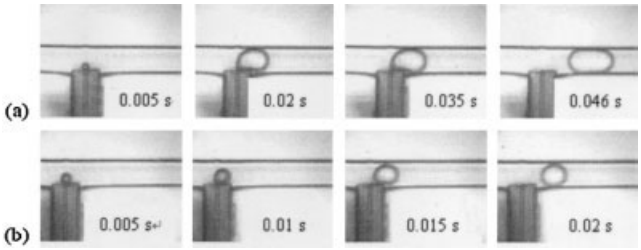

Figure 2. Micrographs of the air–water interface at the intersection channel during bubble-formation processes.

(a) Air-phase flow rate = 25 μL/min, aqueous phase flow rate = 80 μL/min; (b) air-phase flow rate = 25 μL/min; aqueous phase flow rate = 180 μL/min.

ditions. At a low aqueous-phase flow rate of 80 μL/min, the continuous shear force was low and induced the air phase to isolate slugs only because their diameters were greater than the microchannel width. When we increased the aqueous-phase flow rate (Q_L) to 180 μL/min, microbubbles as spheres could be observed. Thus, we could conveniently obtain regular air-water slugs and bubble flow patterns by varying two-phase flow rates.

Then, we investigated the microbubble size and its distribution under different experimental conditions. Figure 3 shows the micrographs of monodispersed microbubbles formed under different experimental conditions. The formed microbubbles had spherical shape with regular size. Figure 4 shows the bubble size distributions and Table 2 shows the values of average bubble size (d_{av}) and polydispersity index (σ) under different experimental conditions. The microbubble size was highly uniform and σ values were $<2\%$ for all of our experimental results, whereas in conventional bubble-formation methods using nozzle, orifice, stirring, and so on, σ values are normally much greater than 2%.

The previous studies for liquid–liquid systems also show that the droplet size is affected by viscosity, interfacial tension, two-phase flow rates, and wetting properties.[9,14-16] Thus the bubble formation is similar to the droplet-formation process using the crossflowing rupture technique in the microfluidic device. Therefore, we investigated in detail the effects of two-phase flow, continuous-phase viscosity, and surfactants on the average microbubble size.

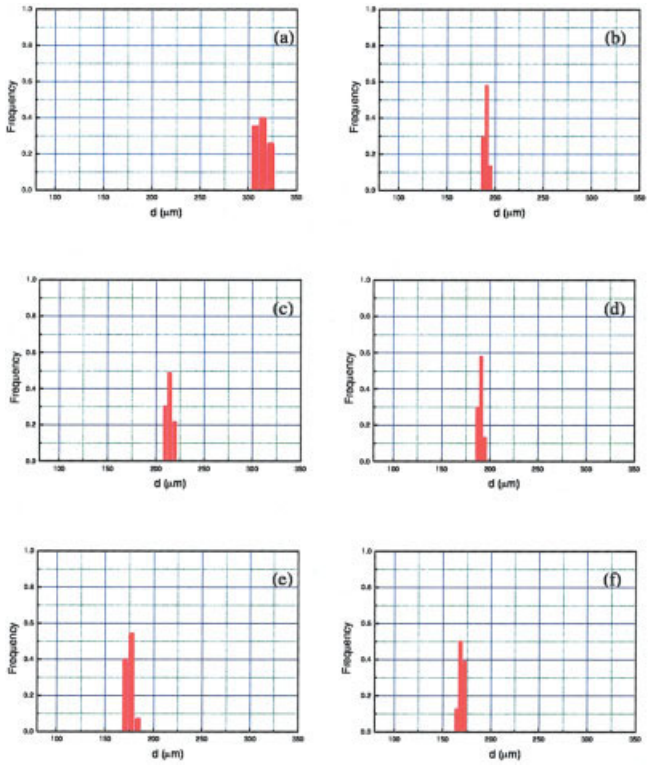

Figure 4. Bubble sizes distribution under different experimental conditions.

The physical properties and experimental conditions are listed in Table 2. [Color figure can be viewed in the online issue, which is available at www.interscience.wiley.com.]

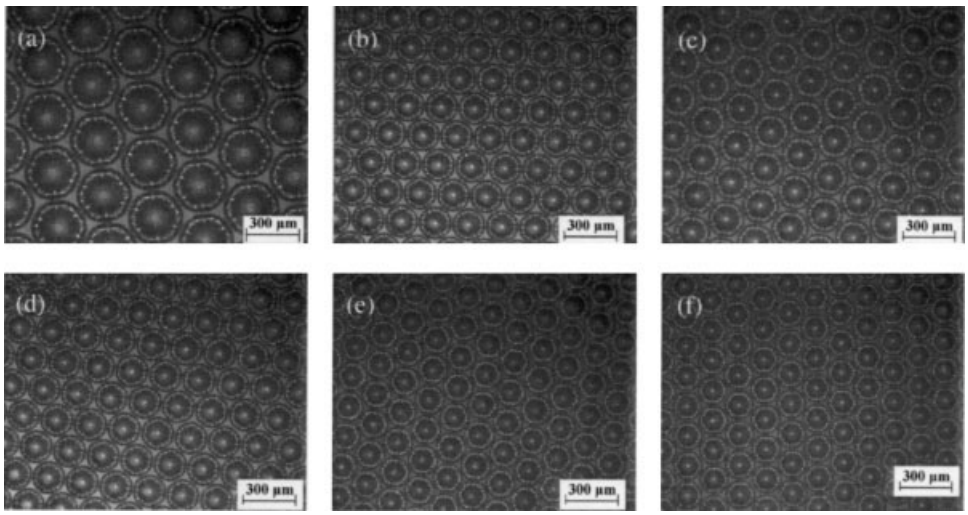

Figure 3. Micrographs of monodispersed microbubbles formed under different experimental conditions.

The physical properties and experimental conditions are listed in Table 2.

Table 2. Comparison of Formed Microbubble Sizes and Distributions under Different Physical Properties of Continuous Phases and Two-Phase Flow Rates

No.	Continuous Phase	Surface Tension, γ (mN m^{-1})	Viscosity, μ (mPa · s)	$Q_g : Q_L$* (μL min^{-1})	Average Bubble Size d_{av} (μm)	σ (%)
(a)	0.5% SDS/water	31.0	0.92	50:100	310.1	1.7
(b)	0.5% SDS/water	31.0	0.92	50:500	189.5	1.3
(c)	0.5% SDS/water	31.0	0.92	200:500	212.7	1.4
(d)	0.05% SDS/water	41.2	0.92	50:500	190.0	1.3
(e)	2% Tween 20/water	37.0	0.92	50:500	174.4	1.8
(f)	0.5% SDS/24% glycerol aqueous solution	30.3	2.0	50:500	168.6	1.4

Q_g, air-phase flow rate; Q_L, aqueous-phase flow rate.

Effects of two-phase flow rates and continuous-phase viscosity on bubble size

Figure 5 shows the effects of two-phase flow rates on bubble size when the continuous phase of 0.5 wt % SDS aqueous solution was applied. The bubble size decreased with increasing continuous-phase flow rate under a certain air-phase flow rate, and the bubble size increased slightly as the air-phase flow rate increased. The bubble size also decreased with increasing continuous-phase flow rate under a certain phase ratio (Q_g/Q_L). Figure 6 shows the effect of the continuous-phase viscosity on the average bubble size when the continuous phases contained different concentrations of glycerol with 0.5 wt % SDS. The continuous-phase viscosities ranged from 0.92 to 10.84 mPa·s. The average bubble size also decreased with increasing continuous viscosity. These results are similar to droplet-formation processes in T-shaped microfluidic devices.[14,16]

Effects of surface tension and surfactants on bubble size

We investigated the effect of surface tension on microbubble size by changing SDS concentrations. Figure 7 shows the effect of surface tension on bubble size under different continuous flow rates. The average microbubble sizes were independent of surface tension, ranging from 55.0 to 31.0 mN/m (range of SDS concentrations: 0.01–0.5 wt %). These results, although different from droplet-formation processes in T-shaped microfluidic devices,[9,14-16] are nonetheless similar to the microbubble-formation processes using the techniques of both flow-focusing rupture[17-19] and geometry-dominated breakup.[20]

Furthermore, we investigated the effect of surfactants on the microbubble size formed by using Tween 20 with concentrations of 1.0 and 2.0 wt % as the other surfactant. Table 3 shows the different properties of the continuous phases with different surfactants. Figure 8 shows the effect of surfactants on bubble size under different continuous flow rates when the air-phase flow rate was 50 μL/min. The average bubble sizes were almost identical in different surfactant concentrations when the same surfactant was applied. However, it was found that the bubble sizes formed by using Tween 20 or SDS as the surfactant were considerably different. Bubble sizes with Tween 20 as the surfactant were smaller than those with SDS, even though they have similar surface tensions. The primary reasons for this difference may lie in the surface wetting and dynamic interfacial properties.

Comparison of the three different monodisperse microbubble-formation mechanisms

Monodisperse microbbules can be prepared by using three different techniques: (1) geometry-dominated breakup, (2) hydrodynamic flow focusing through a small orifice, and (3) crossflowing rupture in a T-junction microchannel. However, the bubble-formation mechanisms are very different in these techniques. In flow-focusing devices (FFDs), the volume V_b of

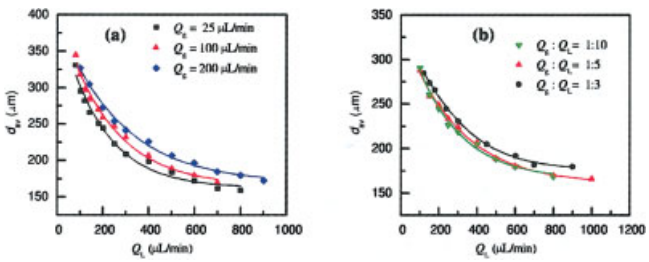

Figure 5. Effects of two-phase flow rates on microbubble size.

The continuous phase was 0.5 wt % SDS aqueous solution in these experiments; the surface tension γ = 31.0 mN/m; continuous phase viscosity μ = 0.92 mPa·s. [Color figure can be viewed in the online issue, which is available at www.interscience.wiley.com.]

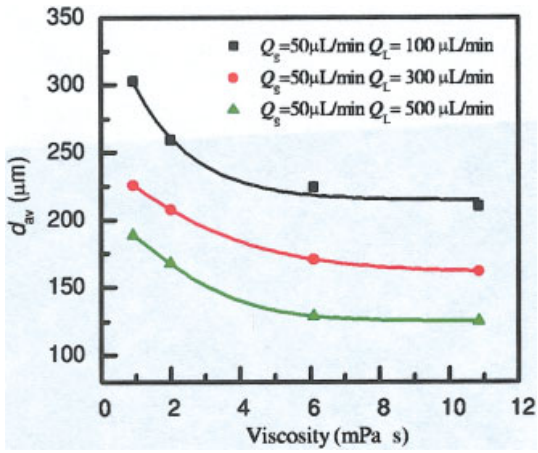

Figure 6. Effect of continuous phase viscosity on the average microbubble size in different continuous phase flow rates when the continuous phases constituted different concentrations of glycerol.

Glycrol concentrations of 24, 52, and 62 wt % were used, respectively. [Color figure can be viewed in the online issue, which is available at www.interscience.wiley.com.]

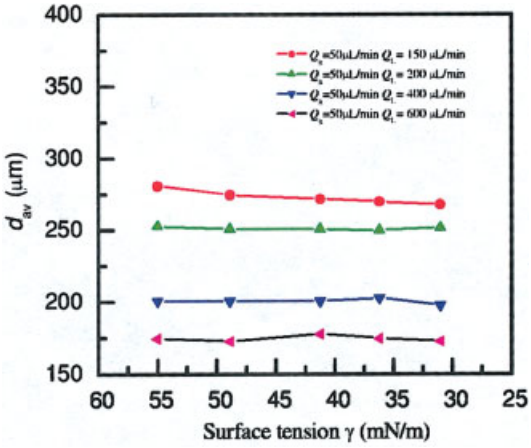

Figure 7. Effect of surface tension on the average microbubble size in different two phase flow rates when the continuous phases constituted different concentrations of SDS solutions.

SDS concentrations of 0.01, 0.02, 0.05, 0.3, and 0.5 wt % were used, respectively. [Color figure can be viewed in the online issue, which is available at www.interscience.wiley.com.]

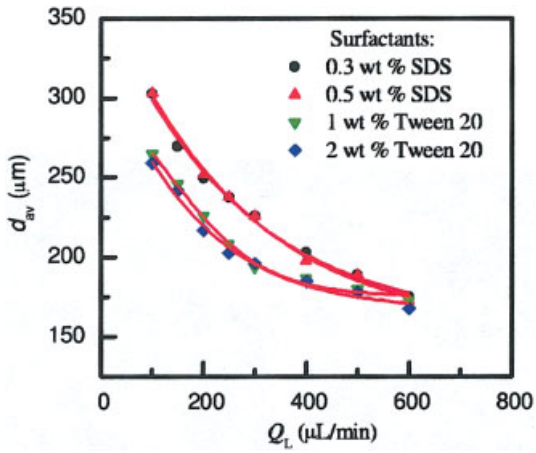

Figure 8. Effect of surfactants on the average microbubble size in different continuous phase flow rates when the continuous phases constituted different concentrations of SDS and Tween 20.

SDS concentrations of 0.3 and 0.5 wt % and Tween 20 concentrations of 1.0 and 2.0 wt % were used, respectively. The air phase flow rate contained 50 μL/min. [Color figure can be viewed in the online issue, which is available at www.interscience.wiley.com.]

the bubbles scaled with the flow rate of the liquid Q_L and the flow rate of the gas stream Q_g as $V_b \propto Q_g/Q_L$, whereas the continuous-phase viscosity μ_c and surface tension γ had no effect on bubble size.[17-19] Microbubble formation by using the technique of geometry-dominated breakup appears to be based on the spontaneous transformation caused by surface tension. The bubble size increased with increasing continuous-phase viscosity, but independent of surface tension and flow rate.[20] In the microbubble-formation process using the crossflow rupture technique, bubble sizes decreased with increasing continuous-phase rate and continuous-phase viscosity, but also independent of surface tension. In all three bubble-formation processes, surface tension did not influence average bubble size, but continuous-phase viscosity and two-phase flow rates had different effects on bubble size. Thus the scaling law of bubble formation by using the crossflow rupture technique is different from that of both hydrodynamic flow focusing and geometry-dominated breakup techniques.

Conclusions

In this work, we first attempted the formation of monodisperse microbubbles using the crossflowing rupture technique in a microfluidic device. The parameters affecting microbubble formation, such as two-phase flow rates, continuous-phase viscosity, surface tension, and surfactant species, were investigated. We also compared the different bubble-formation mechanisms by using the techniques of crossflowing rupture, flow-focusing rupture, and geometry-dominated breakup. We found that bubble sizes decreased with increasing continuous-phase rate and continuous-phase viscosity, but independent of surface tension. The different species of surfactants also influenced the microbubble-formation process because of the variety of wetting properties and dynamic interfacial properties including interfacial viscoelasticity and dynamic interfacial tension. Moreover, the bubble-formation mechanism by using the crossflow rupture technique was different from both the hydrodynamic flow focusing and the geometry-dominated breakup techniques. Understanding of the influences of flow rates, viscosity, contact angle, and wetting property on the dynamics of bubble formation is critical to the theoretical understanding of scaling law of the monodisperse microbubble-formation process in microfluidic devices, thus leading to potential applications in precise control of microbubble sizes in small volumes.

Table 3. Properties of Continuous Phases wit hDifferent Surfactants

Continuous Phase	Surface Tension, γ (mN m^{-1})	Viscosity, μ (mPa · s)
0.5 wt % SDS/water	31.0	0.92
0.3 wt % SDS/water	36.2	0.92
1 wt % Tween 20/water	39.7	0.92
2 wt % Tween 20/water	37.0	0.92

Acknowledgments

We gratefully acknowledge the financial support of the National Natural Science Foundation of China (Grants 20476050, 20490200, 20525622) and SRFDP (20040003032) for this work. We also thank the Department of Biological Sciences and Biotechnology of Tsinghua University for providing the microfluidic device.

Literature Cited

1. Choung JW, Luttrell GH, Yoon RH. Characterization of operating parameters in the cleaning zone of microbubble column flotation. *Int J Miner Process.* 1993;39:31-37.
2. Grinstaff MW, Suslick KS. Air-filled proteinaceous microbubles: Synthesis of an echo-contrast agent. *Proc Natl Acad Sci USA.* 1991;88:7708-7714.
3. Li B, Tao D, Ou Z, Liu J. Cyclo-microbubble column flotation of fine coal. *Sep Sci Technol.* 2003;38:1125-1140.
4. Skyba DM, Kaul S, Advances in microbubble technology. *Coron Artery Dis.* 2000;11:211-219.

5. Liu RH, Yang J, Pindera MZ, Athavale M, Grodzinski P. Bubble-induced acoustic micromixing. *Lab Chip.* 2002;2:151-157.
6. Chen X, Wu H, Mao C, Whitesides GM. A prototype two-dimensional capillary electrophoresis system fabricated in poly(dimethylsiloxane). *Anal Chem*. 2002;74:1772-1778.
7. Song H, Ismagilov RF. Millisecond kinetics on a microfluidic chip using nanoliters of reagents. *J Am Chem Soc.* 2003;125:14613-14619.
8. Zheng B, Roach LS, Ismagilov RF. Screening of protein crystallization conditions on a microfluidic chip using nanoliter-size droplets. *J Am Chem Soc.* 2003;125:11170-11171.
9. Burns JR, Ramshaw C. The intensification of rapid reactions in multiphase systems using slug flow in capillaries. *Lab Chip.* 2001;1:10-15.
10. Sugiura S, Nakajima M, Iwamoto S, Seki S. Interfacial tension driven monodispersed droplet formation from microfabricated channel array. *Langmuir.* 2001;17:5562-5566.
11. Kawakatsu T, Kikuchi Y, Nakajima M. Regular-sized cell creation in microchannel emulsification by visual microprocessing method. *J Am Oil Chem Soc.* 1997;74:317-321.
12. Anna SL, Bontoux N, Stone HA. Formation of dispersions using "flow focusing " in microchannels. *Appl Phys Lett.* 2003;82:364-366.
13. Xu Q, Nakajima M. The generation of highly monodisperse droplets through the breakup of hydrodynamically focused microthread in a microfluidic device. *Appl Phys Lett.* 2004;85:3726-3728.
14. Thorsen T, Roberts R, Arnold F, Quake S. Dynamic pattern formation in a vesicle-generating microfluidic device. *Phys Rev Lett.* 2001;86: 4163-4166.
15. Dreyfus R, Tabeling P, Willaime H. Ordered and disordered patterns in two-phase flows in microchannels. *Phys Rev Lett.* 2003;90:144505/ 1-4.
16. Nisisako T, Torii T, Higuchi T. Droplet formation in a microchannel network. *Lab Chip.* 2002;2:24-26.
17. Ganan-Calvo AM, Gordillo JM. Perfectly monodisperse microbubbling by capillary flow focusing. *Phys Rev Lett.* 2001;87:274501/1-4.
18. Garstecki P, Gitlin I, Diluzio W, Kumacheva E, Stone HA, Whitesides GM. Formation of monodisperse bubbles in a microfluidic flow-focusing device. *Appl Phys Lett.* 2004;85:2649-2651.
19. Garstecki P, Stone HA, Whitesides GM. Mechanism for flow-rate controlled breakup in confined geometries: A route to monodisperse emulsions. *Phys Rev Lett.* 2005;94:164501/1-4.
20. Yasuno M, Sugiura S, Iwamoto S, Nakajima M, Shono A, Satoh K. Monodispersed microbubble formation using microchannel technique. *AIChE J.* 2004;50:3227-3233.

Manuscript received Aug. 25, 2005, and revision received Feb. 8, 2006.